The Physical Modelling of Cardiac Arrhythmias

Rahul Pandit

Centre for Condensed Matter Theory

Department of Physics

Indian Institute of Science, Bangalore, 560012

Work done with

- T K Shajahan
- Alok Ranjan Nayak
- Sitabhra Sinha
- Ashwin Pande
- Avishek Sen

Publications

- Spiral Turbulence: From the Oxidation of CO on Pt(110) to Ventricular Fibrillation - A. Pande, S. Sinha, and R. Pandit , Journal of Indian Institute of Science, Vol. 79, 31 (1999).
- Spatiotemporal Chaos and Nonequilibrium Transitions in a Model Excitable Medium, A. Pande and R. Pandit , Phys. Rev. E, Vol. 61, 6448 (2000).
- Defibrillation via the Elimination of Spiral Turbulence in a Model for Ventricular Fibrillation, S. Sinha, A. Pande and R. Pandit , Phys. Rev. Lett., Vol. 86, 3678 (2001).
- Spiral Turbulence and Spatiotemporal Chaos: Characterization and Control in Two Excitable Media, R. Pandit , A. Pande, S. Sinha, and A. Sen, Physica A, Vol. 306, 211 (2002).

Publications

- Ventricular Fibrillation in a Simple Excitable Medium Model of Cardiac Tissue, T.K. Shajahan, S. Sinha, and R. Pandit, International Journal of Modern Physics B, Vol 17, No 29, pp. 5645-5654 (2003).
- Spatiotemporal chaos and spiral turbulence in models of cardiac arrhythmias: an overview, T K Shajahan, Sitabhra Sinha and Rahul Pandit, Proceedings of Indian National Science Academy, 71, A, pp.47-57 (2005).
- Spiral-Wave Dynamics Depends Sensitively on Inhomogeneities in Mathematical Models of Ventricular Tissue, T K Shajahan, Sitabhra Sinha and Rahul Pandit, Phys. Rev. E, 75, 011929 (2007)

Outline

- Motivation
  - Spatiotemporal chaos and its control in cardiac arrhythmias.
  - Effects of conduction inhomogeneities.
- Models for cardiac tissue.
- Suppressing cardiac chaos.
- Numerical simulations of the effects of conduction and ionic inhomogeneities.
- Conclusions.

Motivation

- Cardiac arrhythmias, like ventricular fibrillation (VF), are a major cause of death in industrialised countries.
- VF: associated with broken spiral waves of electrical activation on cardiac tissue.
- Goal: Understand the dynamics of VF in the presence of obstacles and develop low-amplitude defibrillation techniques.

The Heart

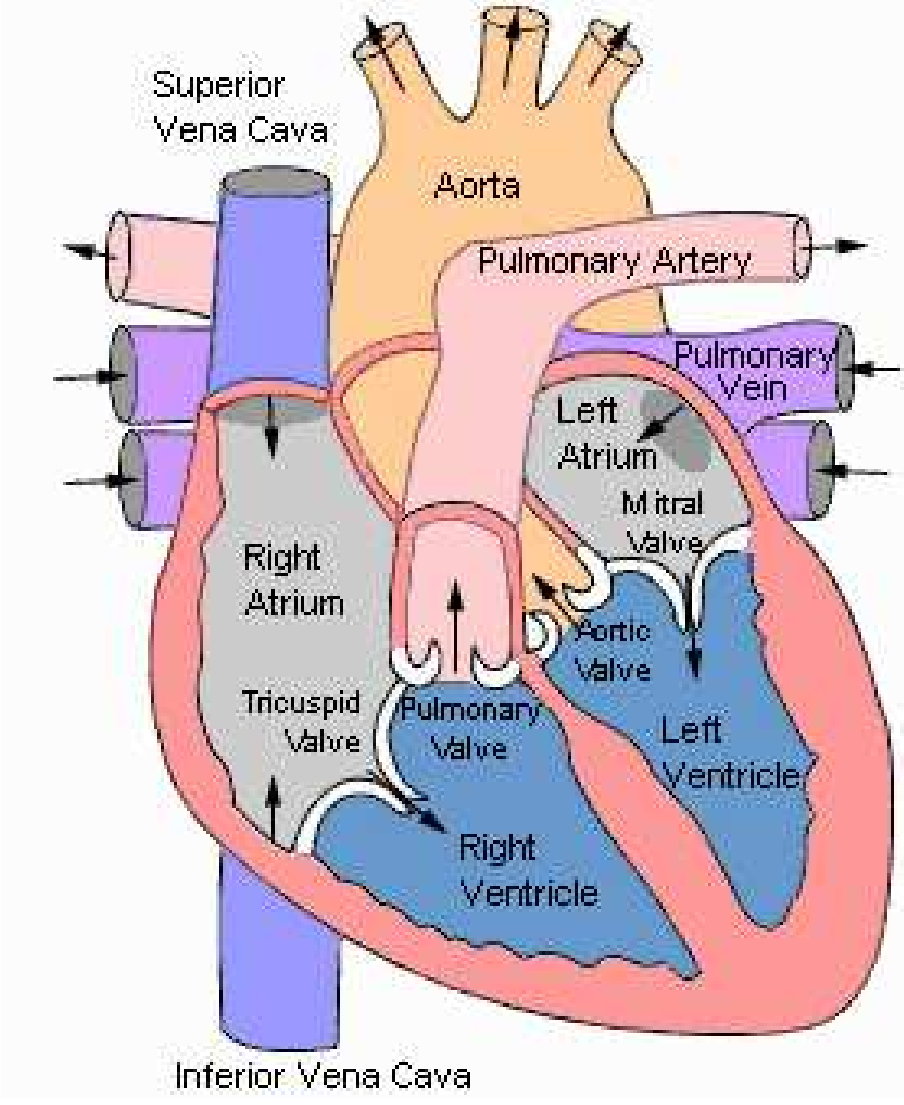
Superior
Vena Cava
Aorta
Pulmonary Artery
Pulmonary
Vein
Left
Atrium
Mitral
Valve
Right
Atrium
Aortic
Valve
Tricuspid
Valve
Pulmonary
Valve
Left
Ventricle
Right
Ventricle
Inferior Vena Cava

The Heart

- One of the most efficient electro-mechanical devices.
- Rhythm: periodic contractions of atria and ventricles.
- For an average adult 72 bpm, i.e., 2.5 billion beats in an average life time.
- The rhythm is maintained by electrical activity in heart muscle.
- VT or VF destroy this rhythm.

Cardiac Arrhythmias

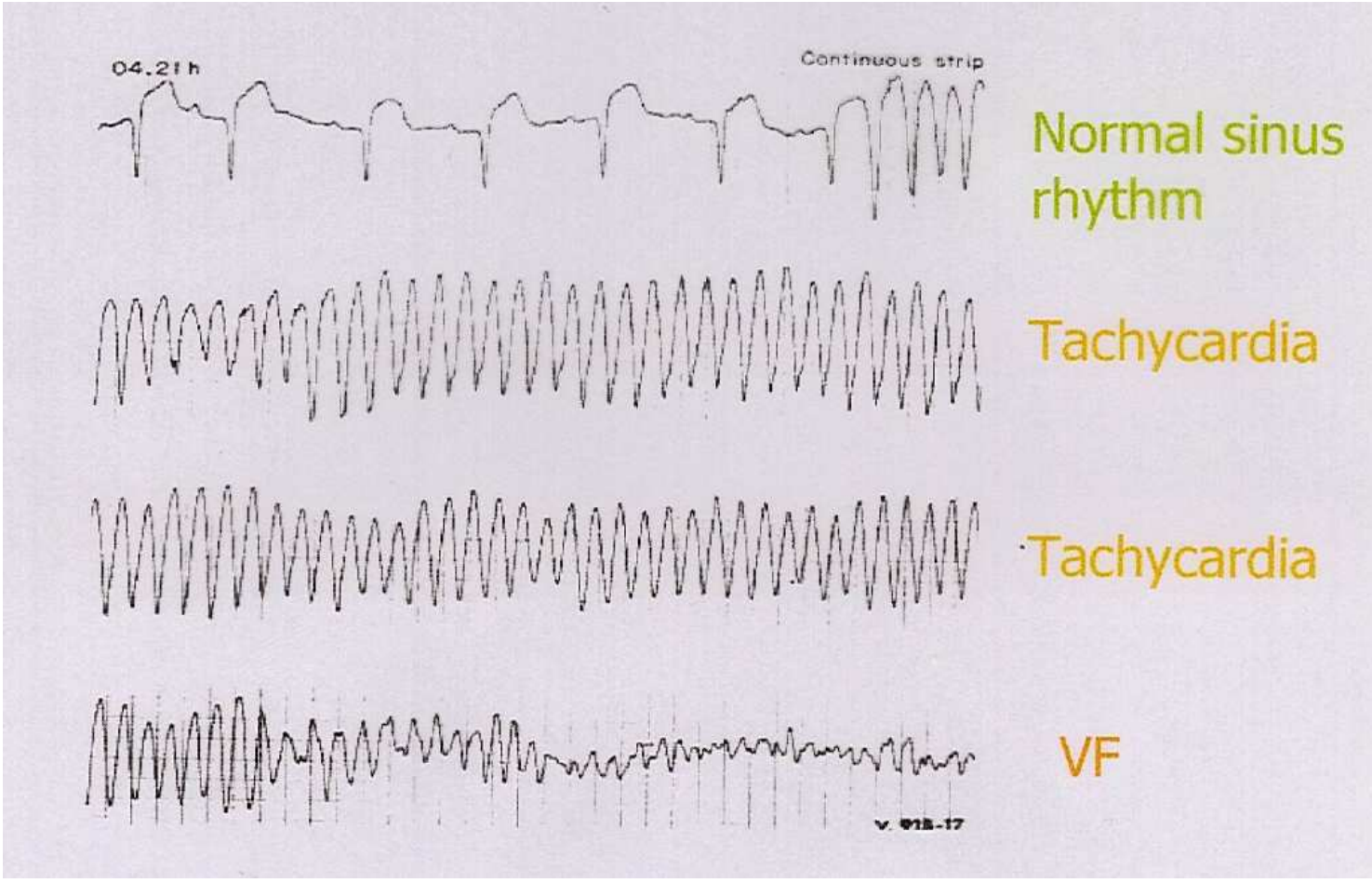

Spiral waves during VF.

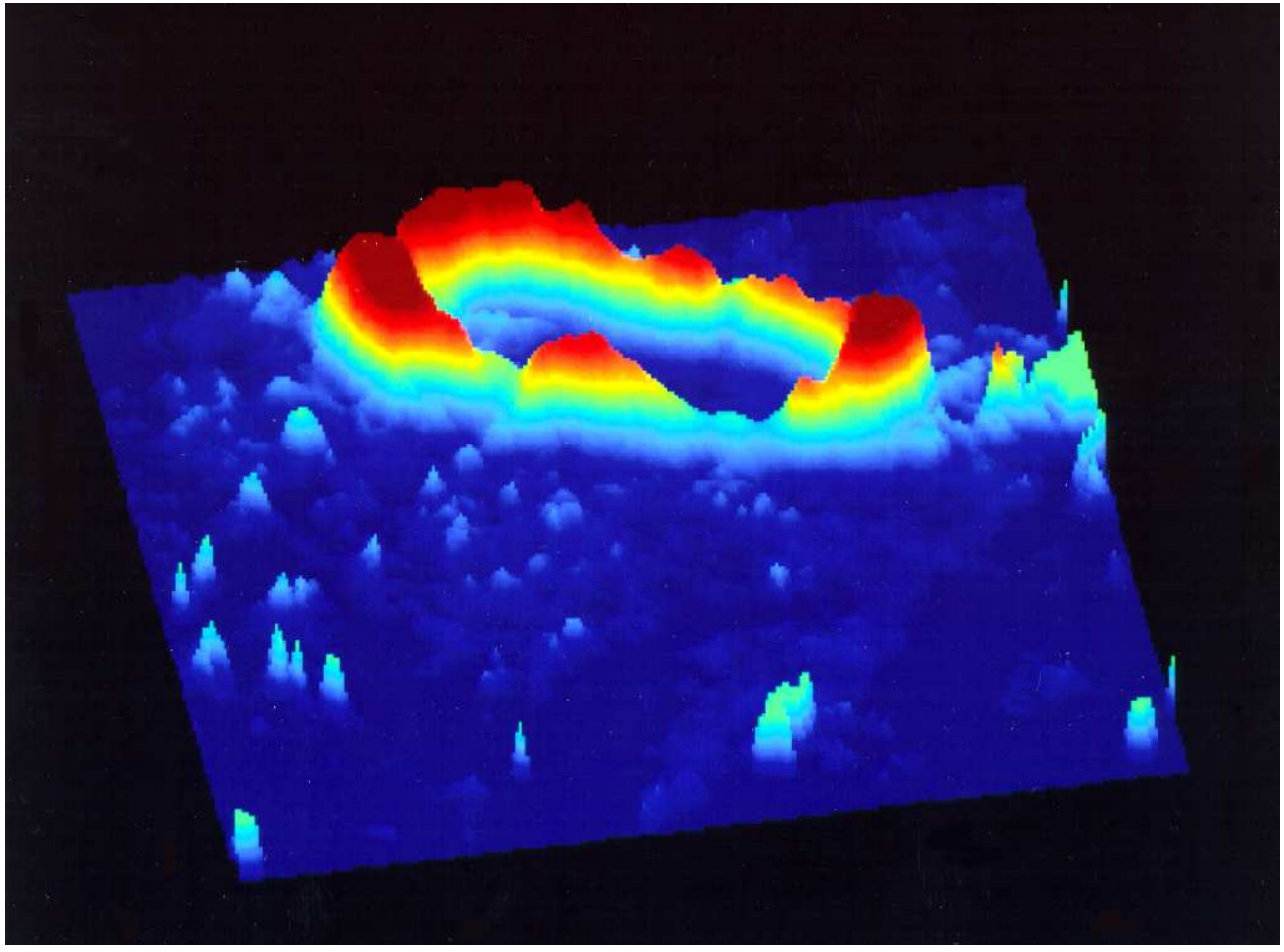

VF in a canine heart imaged via voltage sensitive dyes (from W. Ditto).

Cardiac Cells

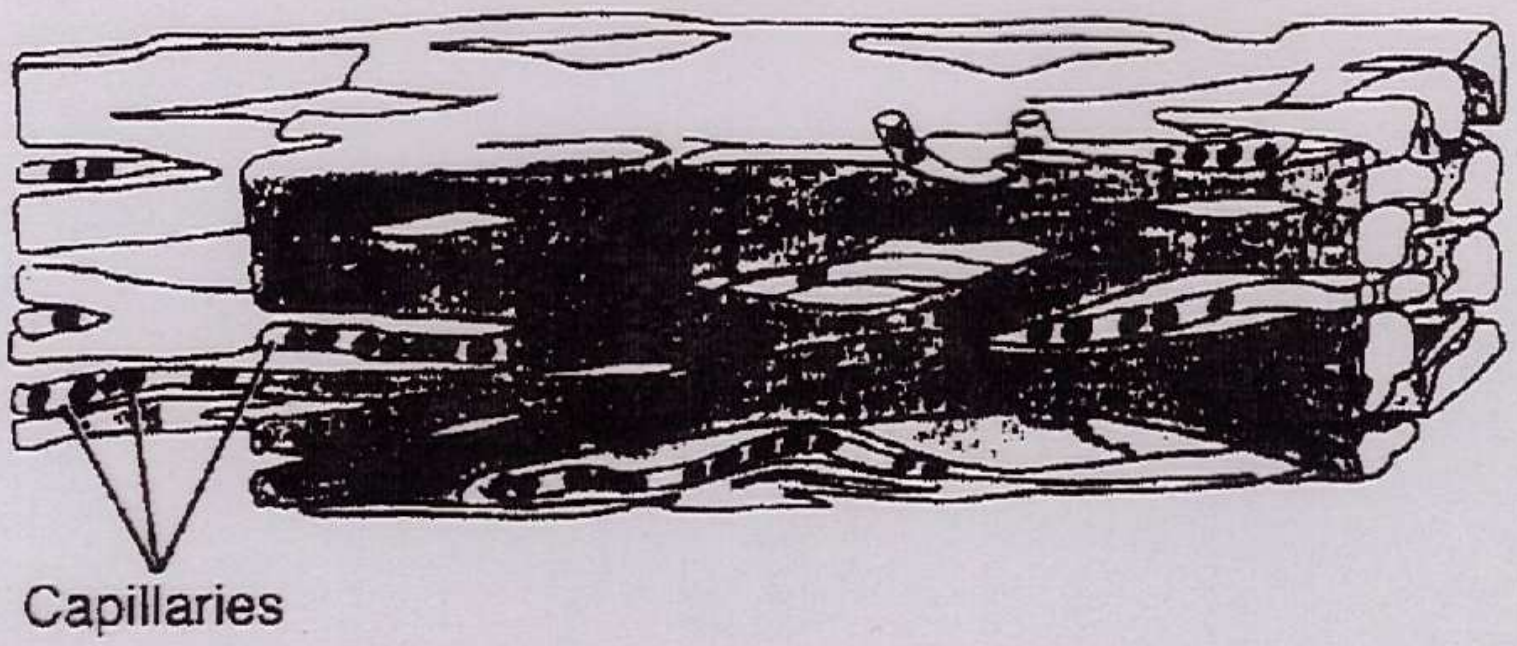

Myocardial fibres: contractile strand of cardiac muscle composed of many cells

Excitability

- Excitation: electrical waves induce cardiac-muscle contractions which pump blood.
- Threshold: the membrane potential of cardiac muscle must exceed ($\simeq$ -60 mV) before the action potential is observed.
- Once excited, cardiac cells cannot be excited further during the refractory period ($\simeq$ 100 ms).

Cardiac Action Potential

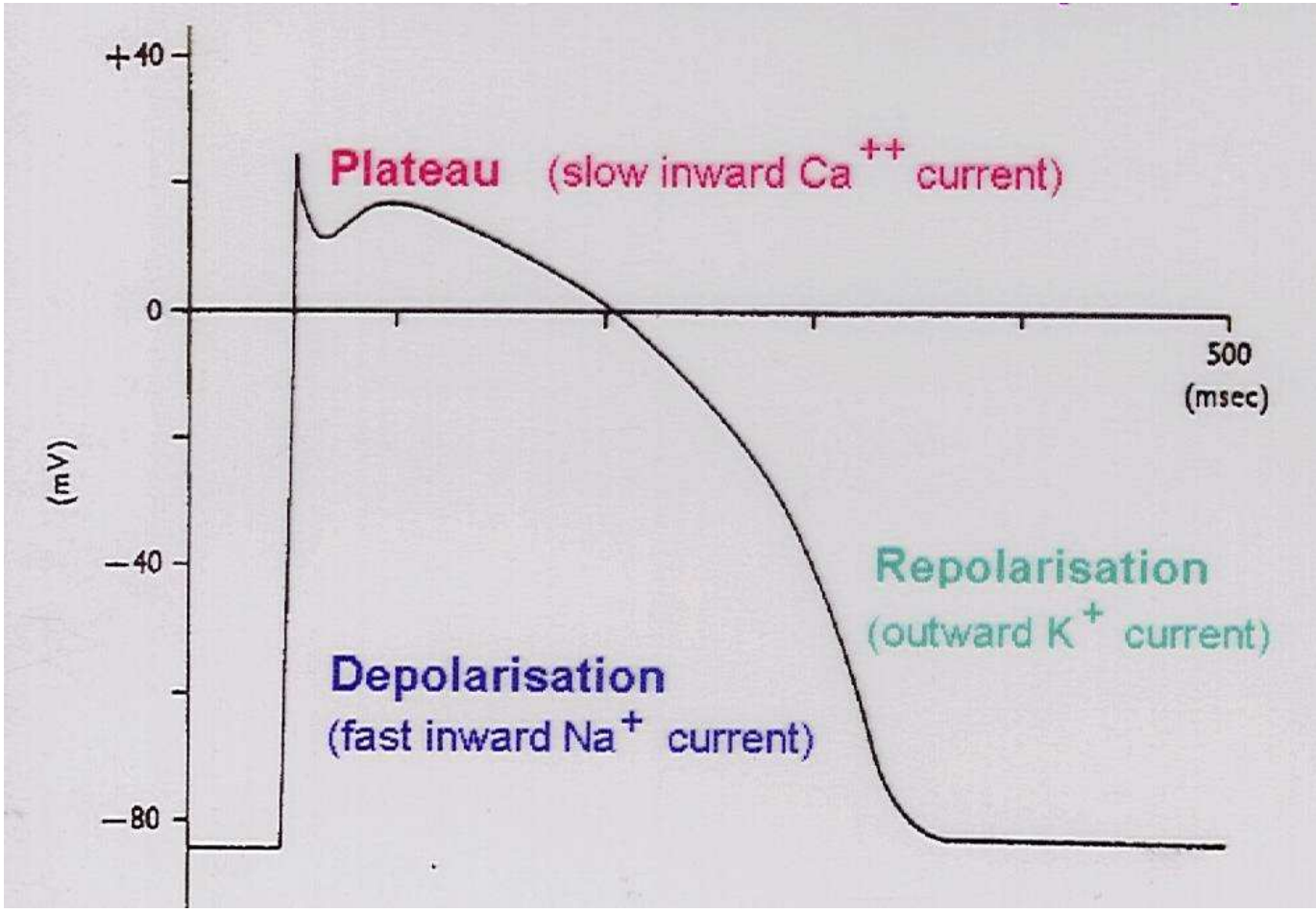

Cardiac Arrhythmias

- They occur when the action potential is abnormally initiated or abnormally conducted.
- They require:
  - a subtrate, i.e., a region of abnormal tissue;
  - a trigger, i.e., an ectopic beat;
  - and possibly other modulating factors.

Cardiac Arrhythmias

- Ectopic beats can arise from metabolic changes inside a cell.
- Reentry or spiral formation can occur because of an anatomical pathway, a single premature stimulus, or a steep restitution of the APD or conduction velocity.

Reentry

Anatomical vs. Functional Reentry

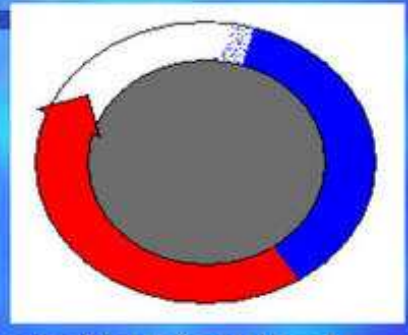

Anatomically determined
(Mines, 1913)

1. Fixed length of circuit (determined by anatomical obstacle).

2. Usually excitable gap between head and tail of impulse.

3. Inverse relation between revolution time and conduction velocity.

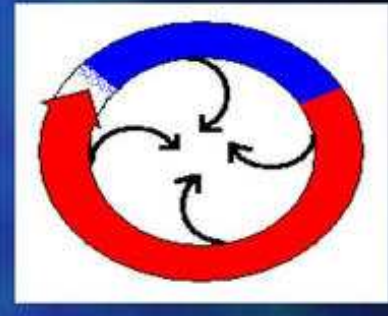

Functionally determined
(Allessie et al., 1977)

1. Circuit length dependent upon electrophysiological properties. ("Spiral waves")

2. No gap of full excitability.

3. Revolution time proportional to length of refractory period.

Underlying Cause of VF

- Formation of electrical vortices
  2D (spiral) or 3D (scroll) waves of action potential that create reentrant pathways of electrical activity.
- Spiral waves lead to an abnormally rapid heart beat ($t \simeq 200$ ms) (Ventricular Tachycardia - VT).
- VT , if untreated, leads to VF in a few seconds through the breakup of spiral wave.

Nonconducting Obstacles

Such inhomogeneities and obstacles, present in cardiac tissue, can yield the following:

- Spiral breakup, i.e., VF.
- Partial suppression, i.e., VF $\rightarrow$ VT transition.
- Complete suppression of VF.

Models of Ventricular Tissue

Basically reaction-diffusion equation of the form

$$\frac{\partial V}{\partial t} + \frac{I}{C} = D\nabla^2 V$$

Various Models; we concentrate on:

- Luo-Rudy Model (realistic);
- Panfilov Model (simplified).

The Panfilov Model

This is the simplest model that shows spiral breakup as in VF; here $e \equiv V$.

$$\begin{aligned} \partial e/\partial t &= \nabla^2 e - f(e) - g, \\ \partial g/\partial t &= \epsilon(e,g)(ke - g). \end{aligned}$$

- $f(e)$: piecewise linear;
- $\epsilon(e,g)$: information about refractory periods.

Panfilov model

$$
\begin{aligned}
f(e) &= C_1 e, e < e_1, \\
f(e) &= C_2 e + a, e_1 \leq e \leq e_2, \\
f(e) &= C_3 (e-1), e > e_2; \\
\epsilon(e,g) &= \epsilon_1, e < e_2, \\
\epsilon(e,g) &= \epsilon_2, e > e_2, \\
\epsilon(e,g) &= \epsilon_3, e < e_1, g < g_1.
\end{aligned}
$$

Numerical Scheme

- Forward Euler in time and finite difference in space.
- Space step δx=0.5 dimensionless units.
- Time step δt=0.022 dimensionless units.
- Dimensioned time T is 5ms times dimensionless time.
- One spatial unit is 1mm. (Ref: A. V. Panfilov and P. Hogeweg, *Phys. Lett. A* **176**, 295 (1993).)

The Luo-Rudy Model

- Biologically realistic model (Luo and Rudy I 1991; II 1994). Incorporates details of ionic currents and ion channels.
- LR I model: 7 coupled ODEs describing the activity of each cardiac cell for the transmembrane potential (V), the intracellular calcium ion concentration (Ca_i), and 9 ion-channel gating variables $m, h, j, X, X_i, d, f, K_1, K_p$.

LR I model

The transmembrane potential V follows a reaction-diffusion equation:

$$\frac{\partial V}{\partial t} + \frac{I_{LR}}{C_m} = D\nabla^2 V$$

$C_m = 1\mu$F/cm^2 is the membrane capacitance, $D(k\Omega^{-1})$ is the conductivity constant and I_{LR} (μA/cm^2) is the instantaneous total ionic current through the cell:

$$I_{LR} = I_{Na} + I_{Si} + I_K + I_{K1} + I_{Kp} + I_b.$$

LR I model: Currents

- Inward currents (Na and Ca) cause depolarization.
- Outward currents (K) cause repolarization.

LR I model: Currents

- This flow of ions through channels in the membrane depends on concentration electrical gradients.
- The Nernst potential at which the chemical and electrical gradients are equal and opposite is

$$E_{ion} = \frac{RT}{nF} \ln \frac{[ion]_o}{[ion]_i}; \tag{1}$$

R : gas constant; T : temperature; n : valence of the ion; F : Faraday's constant; $[ion]_o$ and $[ion]_i$: extra- and intra-cellular ionic concentrations.

LR I model: Currents

The amplitude of an ionic current depends on the conductance of the membrane and the driving force:

$$I_{ion} = \bar{G_{ion}}(V_m - E_{ion}) \quad (2)$$

Conductance $\bar{G_{ion}}$: product of the maximal conductance of all ion channels in the cell (G_{ion}) and the probability ϵ of a channel being in the open state:

$$I_{ion} = G_{ion}\epsilon(V_m - E_{ion}) \quad (3)$$

LR I model: Currents

Inward Currents:

I_{Na}: Fast sodium current

$$I_{Na} = G_{Na} m^3 h j (V - E_{Na})$$

E_{Na}=54.4 mV; I_{Si}: Slow inward current (Ca^{++})

$$I_{Si} = G_{Si} d f (V - E_{Si})$$

$$E_{Si} = 7.7 - 13.0287 \ln([Ca]_i)$$

Ca ion dynamics

The intracellular Ca ion concentration equation:

$$\frac{d[Ca]_i}{dt} = -10^{-4} I_{Si} + 0.07(10^{-4} - [Ca]_i)$$

LR I model: Outward Currents

I_K: Time-dependent potassium current

$$I_K = G_K X X_i (V - E_K)$$

I_{K1}: Time-independent potassium current

$$I_{K_1} = G_{K_1} K_{1\infty} (V - E_{K_1})$$

LR I model: Outward Currents

I_{Kp}: Plateau potassium current

$$I_{K_p} = G_{K_p} K_p (V - E_{K_p})$$

I_b: Background current

$$I_{K_b} = G_{K_b} (V - E_{K_b})$$

Gating Variables

The gating variables m, h, j, d, f, X, and K_1, are the probabilities of the channels being in the open state. They obey ODEs of the form:

$$\frac{d\epsilon}{dt} = \alpha_\epsilon(1-\epsilon) - \beta_\epsilon\epsilon$$

α_ϵ and β_ϵ : rates at which gates open and close.

Gating Variables

Steady-state: $d\epsilon/dt = 0$ yields

$$\epsilon_\infty = \frac{\alpha_\epsilon}{(\alpha_\epsilon + \beta_\epsilon).} \tag{4}$$

$$\epsilon = \epsilon_\infty - (\epsilon_\infty - \epsilon_0)\exp(-t/\tau) \tag{5}$$

$$\tau = 1/(\alpha_\epsilon + \beta_\epsilon) \tag{6}$$

Rate Constants

By measuring the voltage dependences of ϵ and τ and by using the above equations we can obtain α_ϵ and β_ϵ for each value of the membrane potential. These results for α_ϵ and β_ϵ can be fitted to obtain the following relations:

Rate Constants

$$
\begin{aligned}
\alpha_h &= 0, \text{ if } V \geq -40 \text{ mV}, \\
&= 0.135 \ \exp\left[-0.147\ (V+80)\right], \text{ otherwise;} \\
\beta_h &= \frac{1}{0.13\ (1+\exp\left[-0.09(V+10.66)\right])}, \\
&\text{if } V \geq -40 \text{ mV}, \\
&= 3.56 \ \exp\left[0.079\ V\right] + 3.1 \times 10^5 \ \exp\left[0.35\ V\right], \\
&\text{otherwise;}
\end{aligned}
$$

Rate Constants

$$\alpha_j =$$

$$0, \text{ if } V \geq -40 \text{ mV},$$

$$\frac{(\exp[0.2444\ V] + 2.732 \times 10^{-10}\ \exp[-0.04391\ V])}{-7.865 \times 10^{-6}\{1 + \exp[0.311\ (V + 79.23)]\}} \times (V + 37.78),$$

$$\text{otherwise;}$$

Rate Constants

$$\beta_j = \frac{0.3\ \exp\left[-2.535 \times 10^{-7}\ V\right]}{1 + \exp\left[-0.1\ (V + 32)\right]}, \text{if } V \geq -40 \text{ mV},$$

$$= \frac{0.1212\ \exp\left[-0.01052\ V\right]}{1 + \exp\left[-0.1378\ (V + 40.14)\right]}, \text{ otherwise;}$$

Rate Constants

$$\alpha_m = \frac{0.32\ (V + 47.13)}{1 - \exp\left[-0.1\ (V + 47.13)\right]};$$

$$\beta_m = 0.08\ \exp\left[-0.0909\ V\right];$$

$$\alpha_d = \frac{0.095\ \exp\left[-0.01\ (V - 5)\right]}{1 + \exp\left[-0.072\ (V - 5)\right]};$$

$$\beta_d = \frac{0.07\ \exp\left[-0.017\ (V + 44)\right]}{1 + \exp\left[0.05\ (V + 44)\right]};$$

Rate Constants

$$\alpha_f = \frac{0.012 \ \exp\left[-0.008\ (V+28)\right]}{1+\exp\left[0.15\ (V+28)\right]};$$

$$\beta_f = \frac{0.0065 \ \exp\left[-0.02\ (V+30)\right]}{1+\exp\left[-0.2\ (V+30)\right]};$$

$$\alpha_x = \frac{0.0005 \ \exp\left[0.083\ (V+50)\right]}{1+\exp\left[0.057\ (V+50)\right]};$$

$$\beta_x = \frac{0.0013 \ \exp\left[-0.06\ (V+20)\right]}{1+\exp\left[-0.04\ (V+20)\right]};$$

Rate Constants

$$\alpha_{K1} = \frac{1.02}{1+\exp\left[0.2385\ (V - E_{K1} - 59.215)\right]};$$

$$\beta_{K1} = \frac{\left[0.49124\ \exp\left[0.08032\ (V - E_{K1} + 5.476)\right]\right.}{1+\exp\left[-0.5143\ (V - E_{K1} + 4.753)\right]}$$
$$\left.+\exp\left[0.06175\ (V - E_{K1} - 594.31\right]\right].$$

$$X_i = \frac{2.837\ \exp 0.04(V+77) - 1}{(V+77)\exp 0.04\ (V+35)}, \text{if } V > -100\text{mV},$$
$$= 1,\ \text{otherwise};$$

$$K_p = \frac{1}{1+\exp\left[0.1672\ (7.488 - V)\right]}.$$

Initial Condition

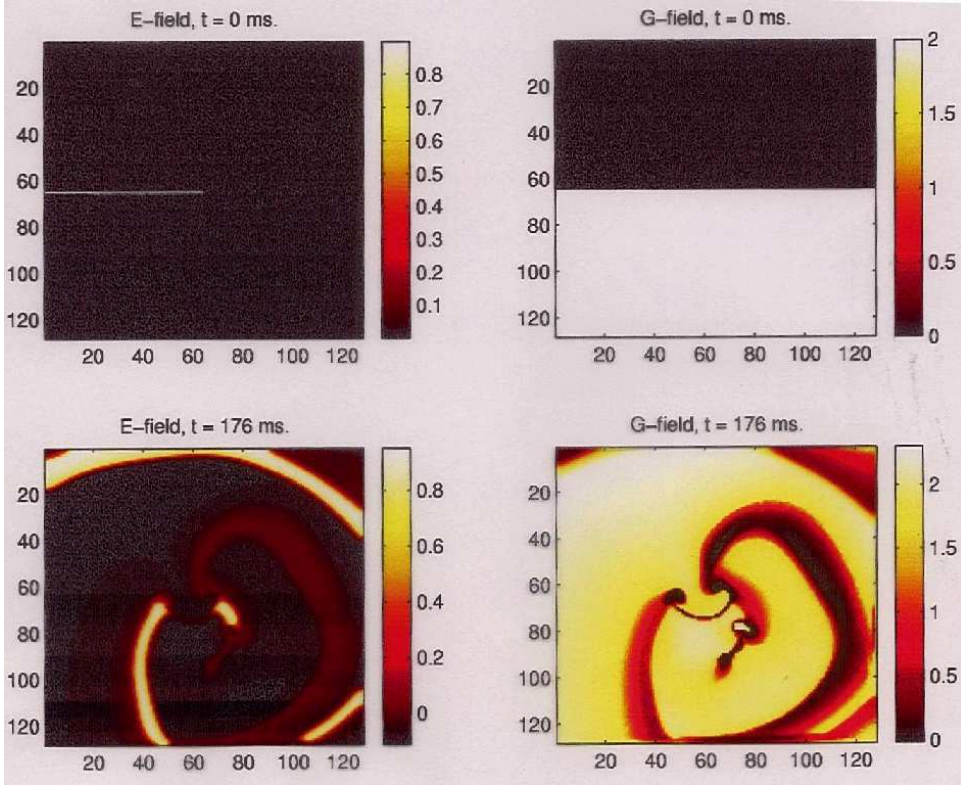

Spiral Turbulence (Panfilov Model)

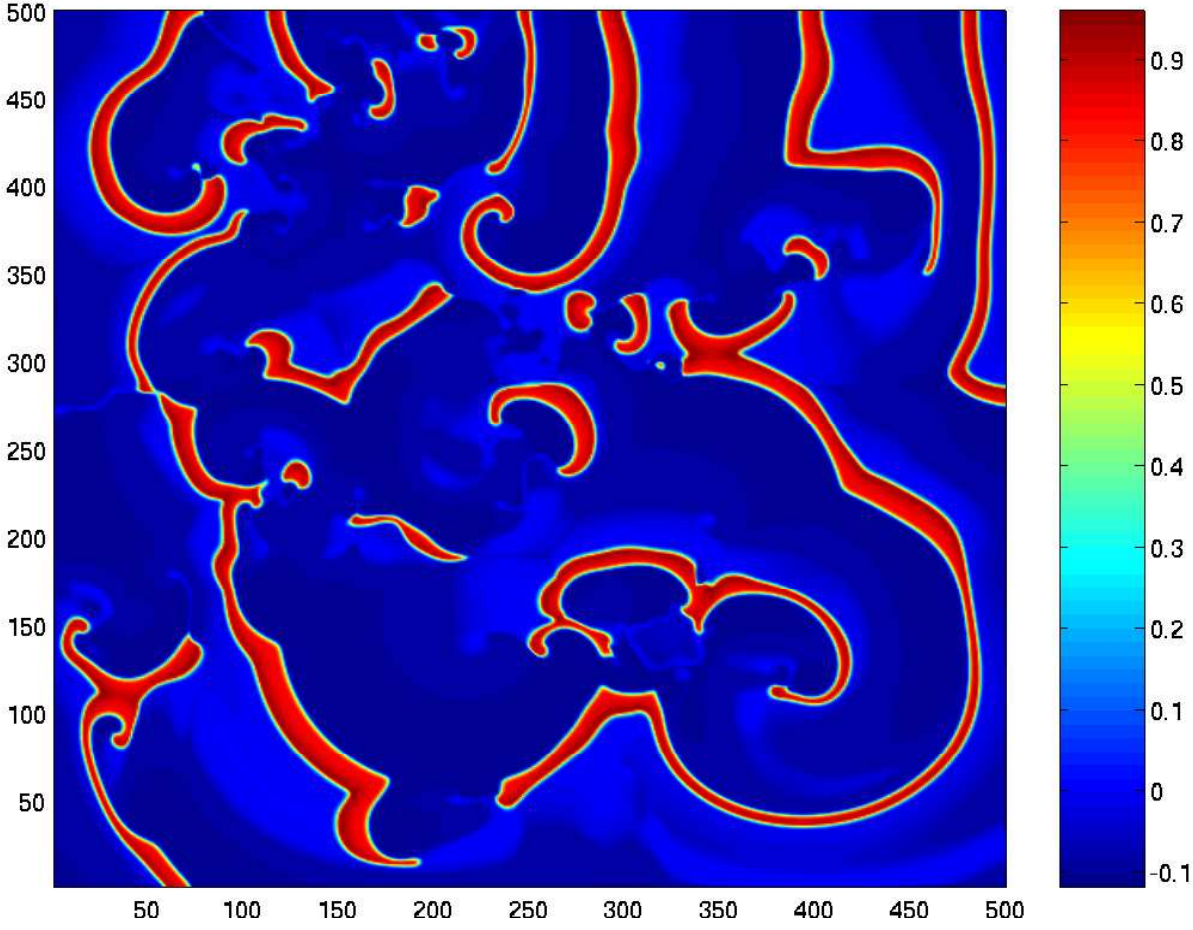

Animation

Spiral Turbulence (Panfilov Model)

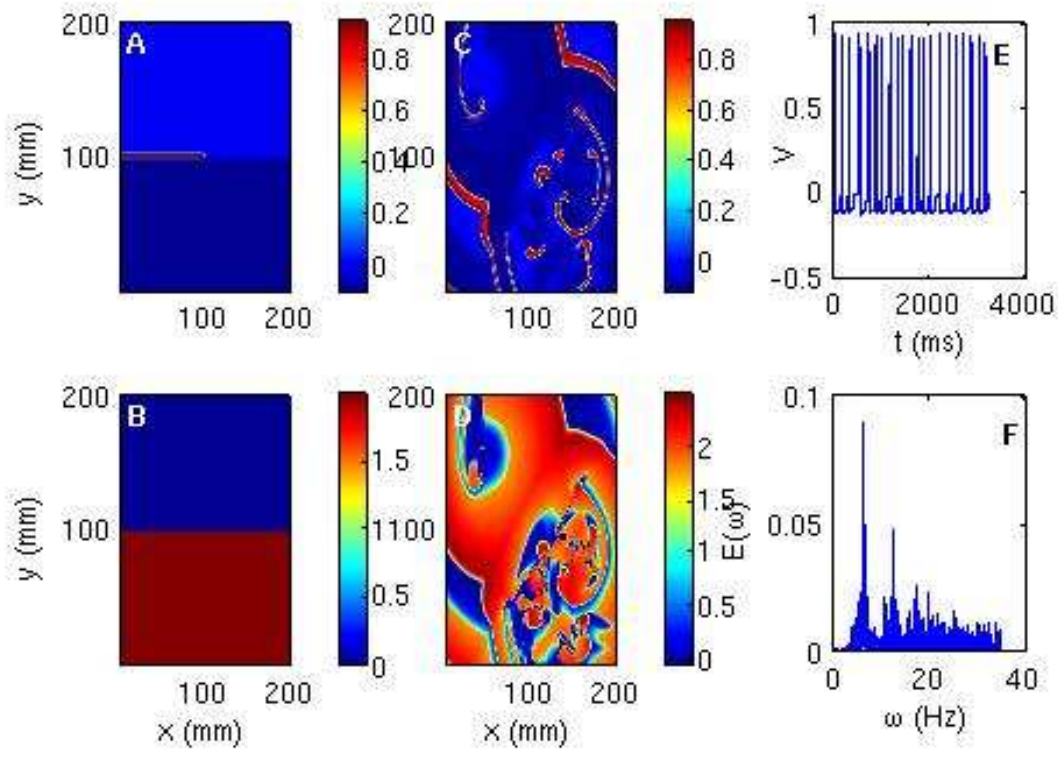

The Initial condition used in the simulation for the field V and g shown in A and B respectively. C and D shows e and g fields after t=2750 ms. Local time series and power spectrum is shown in E and F respectively.

Panfilov Model

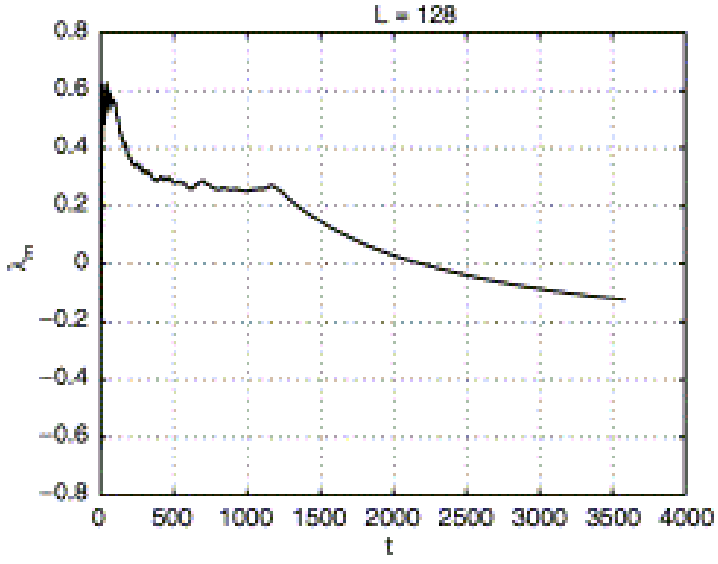

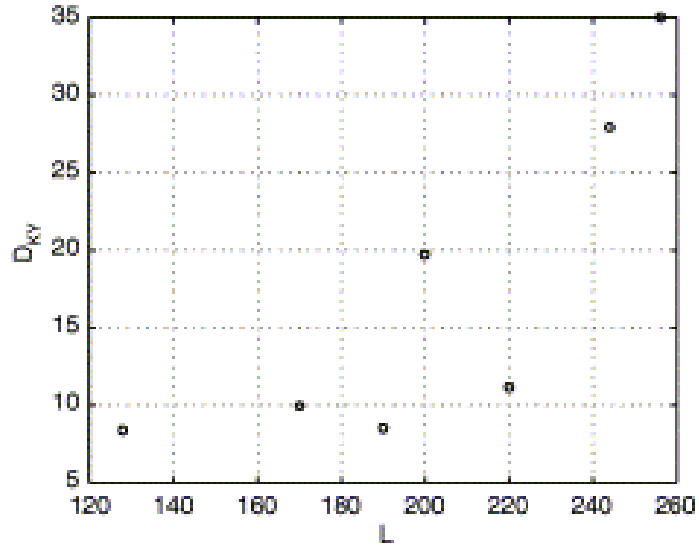

The maximum Lyapunov exponent λ_m at time t versus t (left) for for the Panfilov model. λ_m approaches a positive constant (0.2) and then decays at large times to negative values indicating a long-lived chaotic transient which finally decays to a quiescent state with and everywhere. The Kaplan-Yorke dimension DKY (right) in the spatiotemporally chaotic transient versus the linear system size L.

The Reduced P B Model

- Uses human cell data
- Incorporates ion pumps
- Dynamics similar to, but more complicated than, the LR I model.

LR Model: Numerical Method

- Forward Euler in time and finite difference in space.
- δt=0.01ms, δx=0.0025 cm.
- The resting-state value of V is -84 mV. All gating variables are initialised to their steady-state value, i.e., ϵ_∞.

Initial Conditions

- Initial stimulus: 150 μA/cm^2 at the top boundary for 1ms. This initiates a plane wave.
- Next stimulus: from left boundary at 285 ms after the first stimulus (for 0.45 ms).
- Last stimulus:from the top boundary at 465 ms for 0.45 ms.
- Spiral formation by 665 ms.
- Spiral breakup by 850 ms.

Spiral Turbulence: LR Model

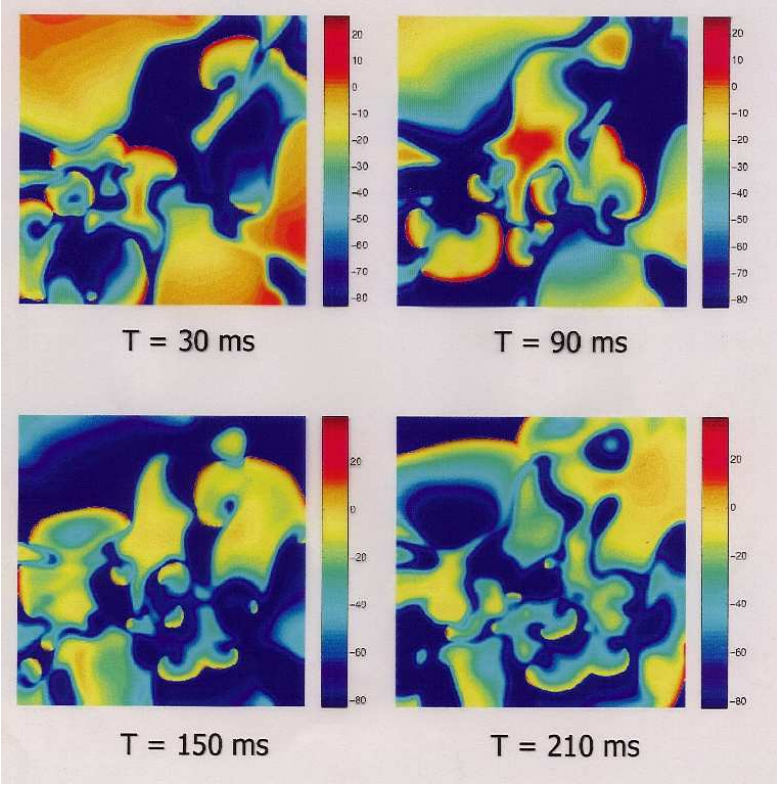

Spiral Turbulence: LR Model

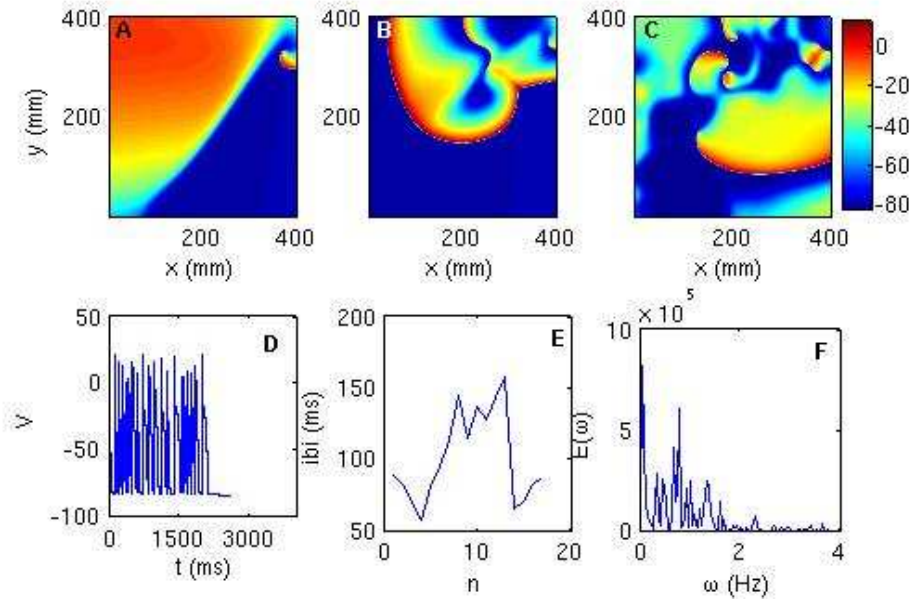

Initial conition used for the simulation of LR I model. The simulation domain is 90×90 mm^2. The initial transmembrane voltage V shown in (A) evolves into (B) after 600 ms and into (C) after 1000 ms. D, E, and F show the local time series, interbeat interval, and powerspectrum calculated from a sample of 261 424 iterations.

Spiral Turbulence: redPB Model

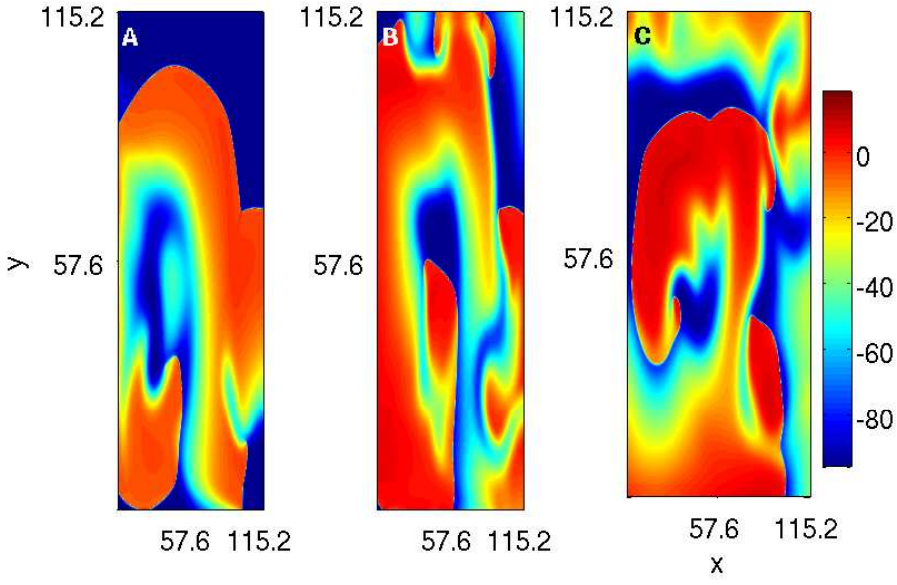

Defibrillation

- Pharmaceutical means: Administer medication ...
- Electrical means:
  - Electrical defibrillation: Two paddles are placed on the chest and a large electric shock ($\sim$ 5 kV) applied across them.
  - Internal defibrillation: Administer electrical shocks (~ 600 V) through an implantable electrical defibrillator which also detects the onset of VF.

Defibrillation

Example of an implantable cardiac defibrillator (ICD)

Vol 54 cc
Mass 97 gm
Thickness 16mm
Longevity 9 yrs
BOL Voltage 6.4 V
ERI 4.91 V
BOL Charge time 6.0 sec

Defibrillation

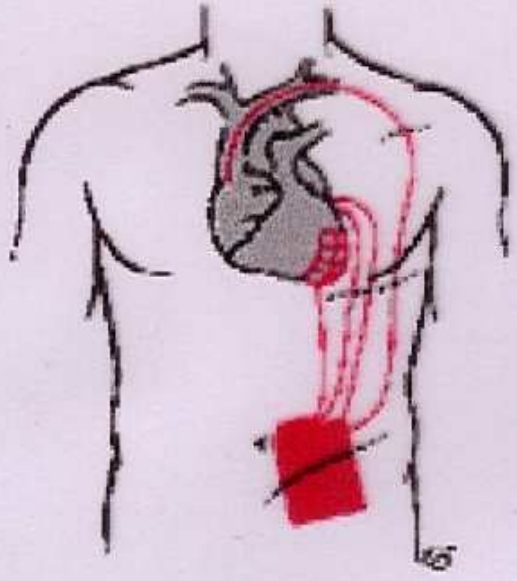

An internal defibrillating system consists of a pulse generator and electrical leads. Endocardial leads are inserted into the venous system, usually via the subclavian or cephalic vein and advanced to the right ventricle and/or atrium. The pulse generator is placed subcutaneously or submuscularly and connected to the leads.

Control in 2-D Models

- The models have non-conducting boundaries (*no-flux* or *Neumann* boundary conditions): ventricles are electrically insulated from atria. Observations:
- Non-conducting boundaries absorb spiral defects.
- Spirals do not last for appreciable periods in small systems.

Operating Principles

- Divide the system ($L \times L$) into K^2 smaller blocks.
- Isolate the blocks (size L/K) by stimulating the system along the block boundaries - making them refractory.

Operating Principles

- Each block is too small to sustain spiral activity - spirals absorbed by block boundaries.
- After the system is driven to the quiescent state, controlling stimulation is withdrawn- block boundaries recover from refractory state.

Without Control

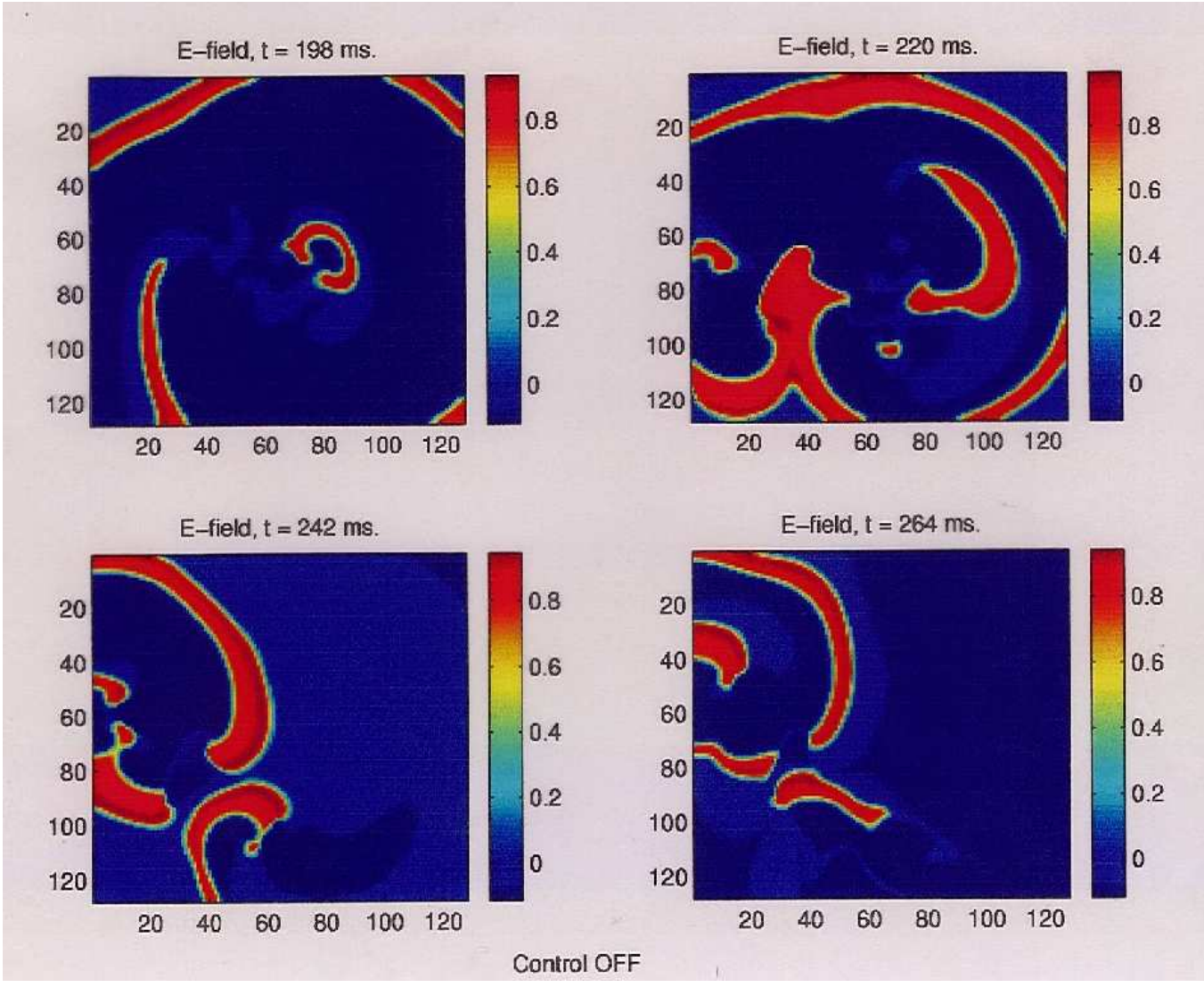

Control ON

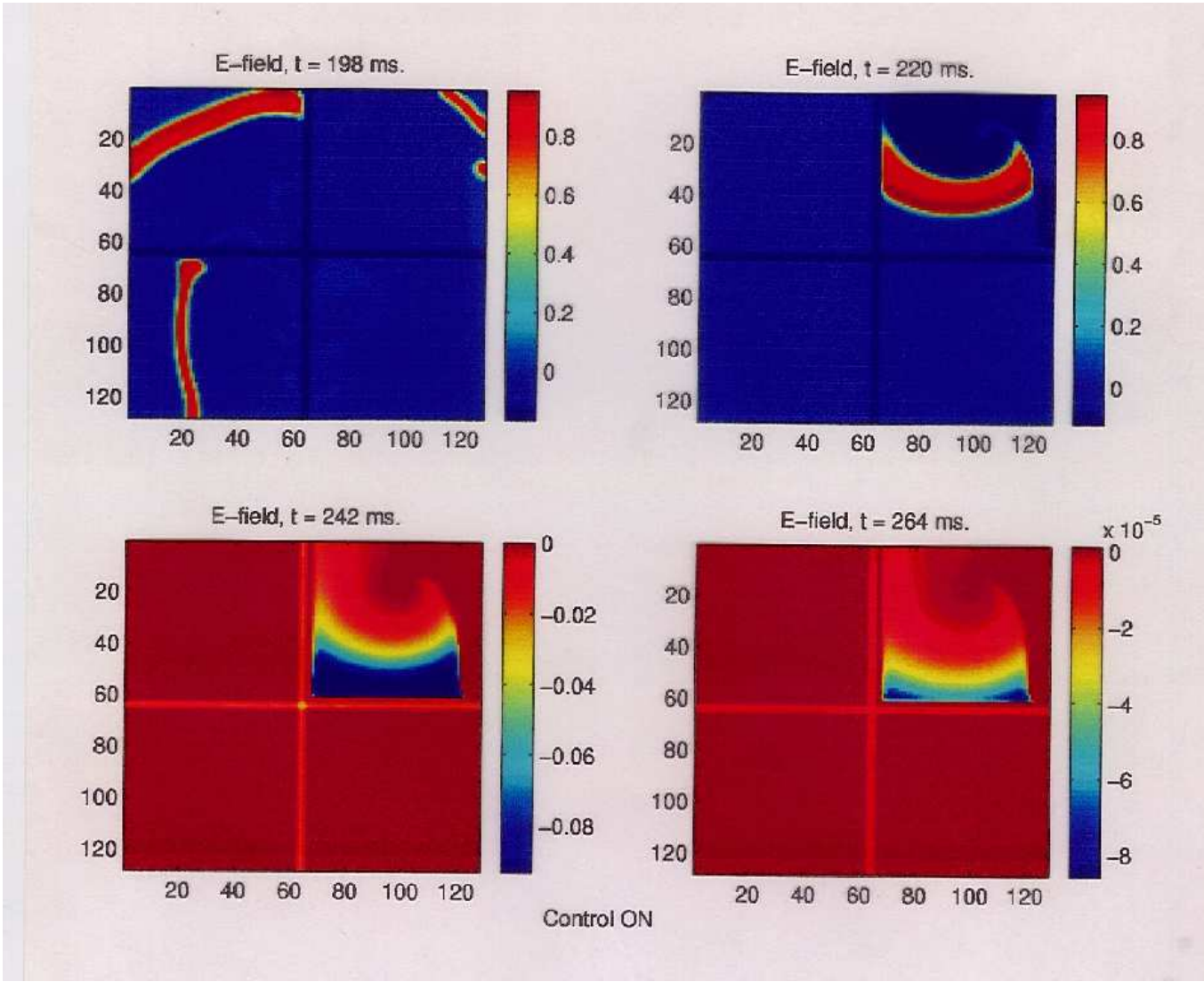

Animation

Control Parameters in 2-D

- Panfilov Model
  L = 256
  Pulse amplitude $\simeq$ 57.3 mV/ms.
  Kept on for τ = 41.2 ms.
  This implies a defibrillation current density of 57 μ A/cm^2.

Control in 2-D Panfilov

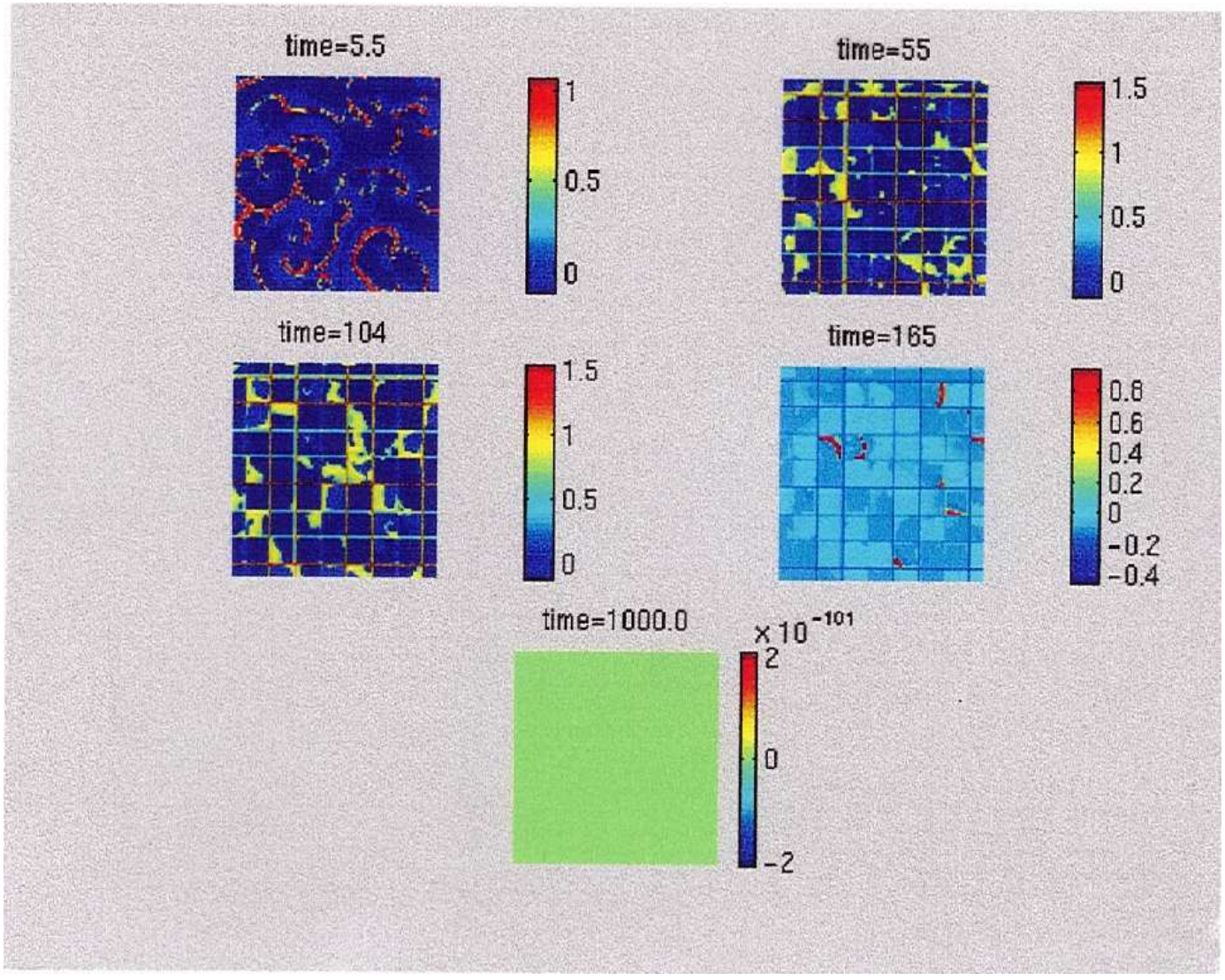

Control in 2-D LR

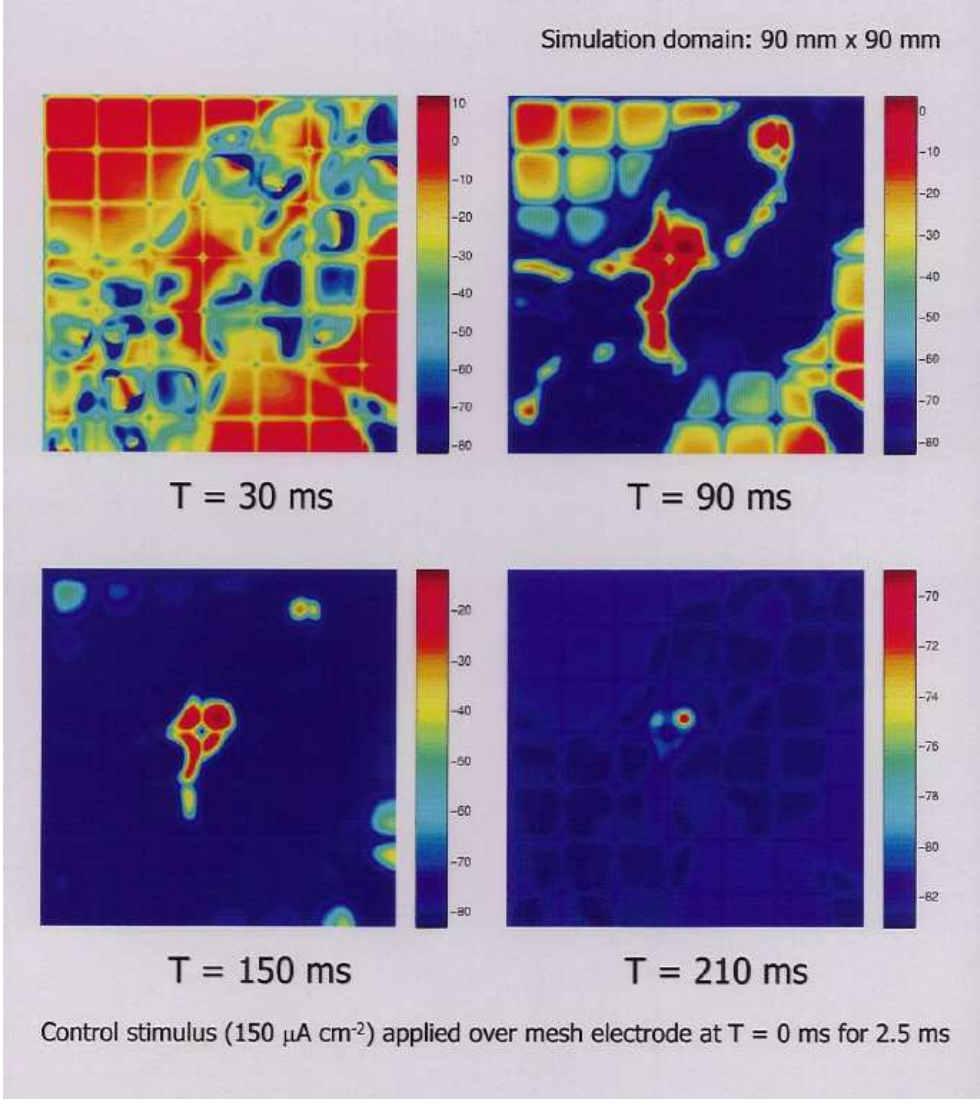

Panfilov Model : Control in 3-D

Control algorithm as in 2-D with the following modifications:

- Control mesh only on free face of a 3-D domain ($L \times L \times L_z$).
- With L = 256 control obtained for L_z.

Panfilov Model : Control in 3-D

For $L_Z >$4 pulsed control is necessary:

- activate control mesh after τ ms;
- keep it on for τ_{ON} ms;
- turn it off for τ_{OFF} ms;
- keep it on for τ_{ON} ms;
- repeat n times.
  We find τ_{ON}=0.11 ms, τ_{OFF}=22 ms and $n = 30$ suffices. τ_{OFF} is comparable to the duration of one action potential.

3D Control

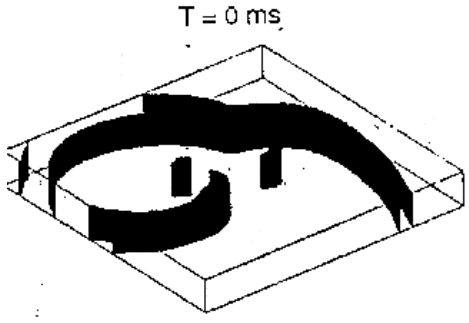

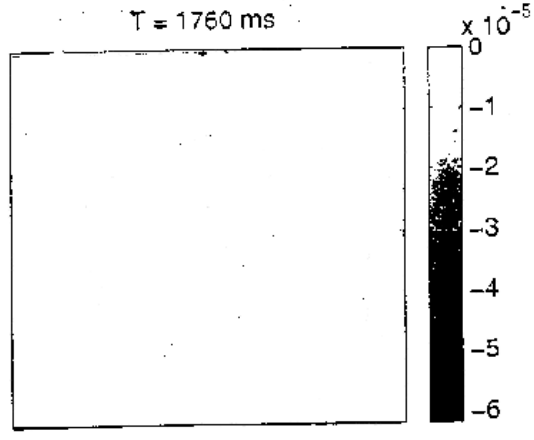

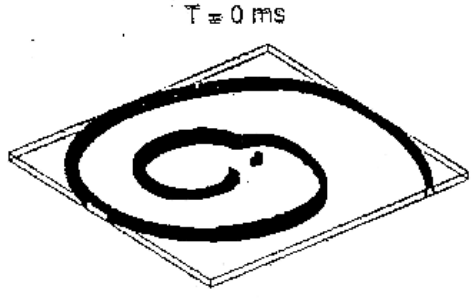

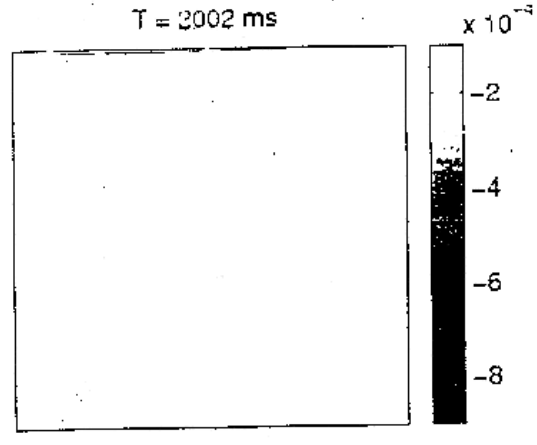

Nonconducting Obstacles

In our models we have introduced nonconducting inhomogeneities (say 80×80 in a 400×400 simulation domain) and we find all the three types of behaviours mentioned above:

- Sometimes the inhomogeneity causes spiral breakup (red).
- Sometimes it suppresses VF partially and converts it into VT (blue).
- It can even suppress VF completely (green).

Obstacle: Panfilov Model, ST

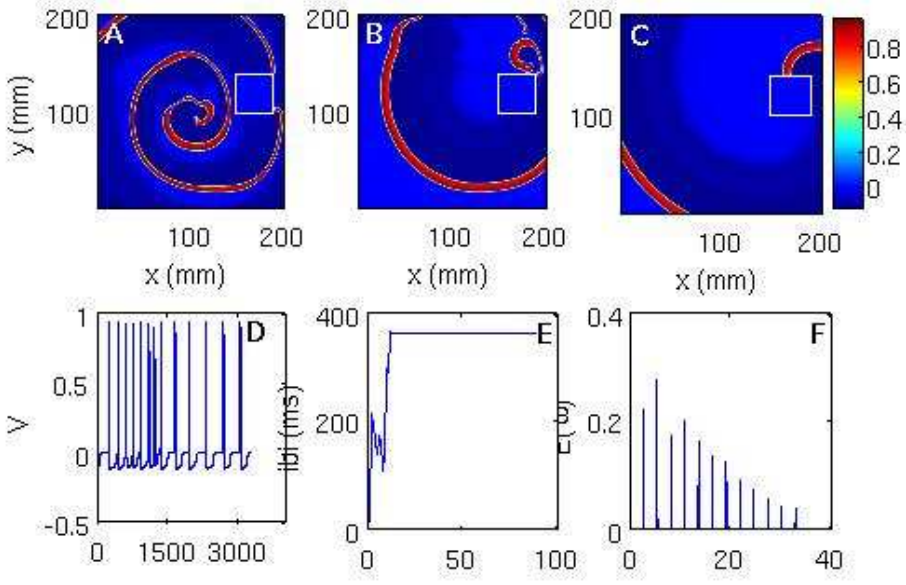

When an obstacle of side 40 mm is placed at (x =100 mm, y=160 mm) the spiral breaks up. A, B and C shows snapshots at time 1100 ms, 1650 ms and 2750 ms respectively. The local time series, interbeat interval IBI,and power spectrum of the transmembrane potential e(x,y,t) are shown in D, E, and F respectively.

Obstacle: Panfilov Model, RS

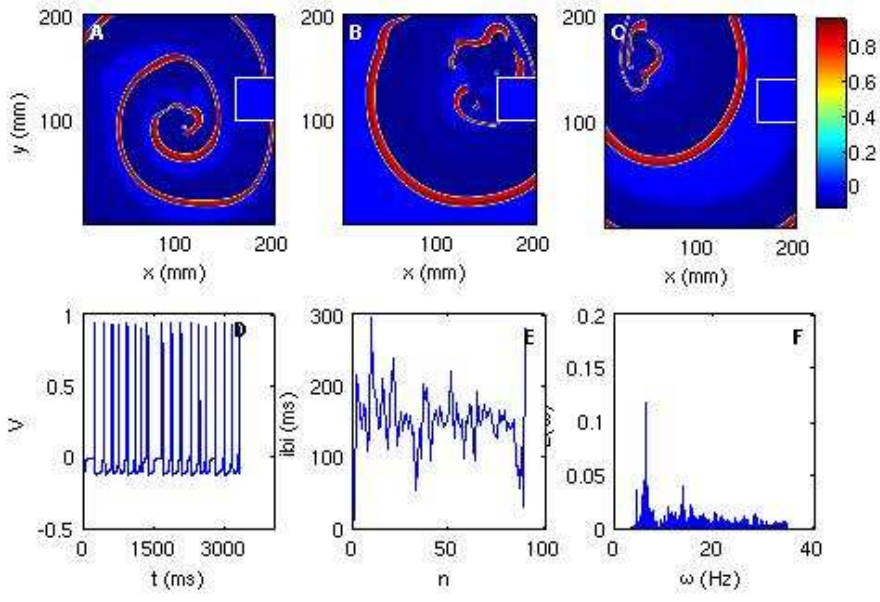

When an obstacle of side 40 mm is placed at (x =100 mm, y=150 mm) the spiral gets attached to it. A, B and C shows snapshots at time 1100 ms, 1650 ms and 2750 ms respectively. The wave gets attached to the obstacle.

Obstacle: Panfilov Model, NS

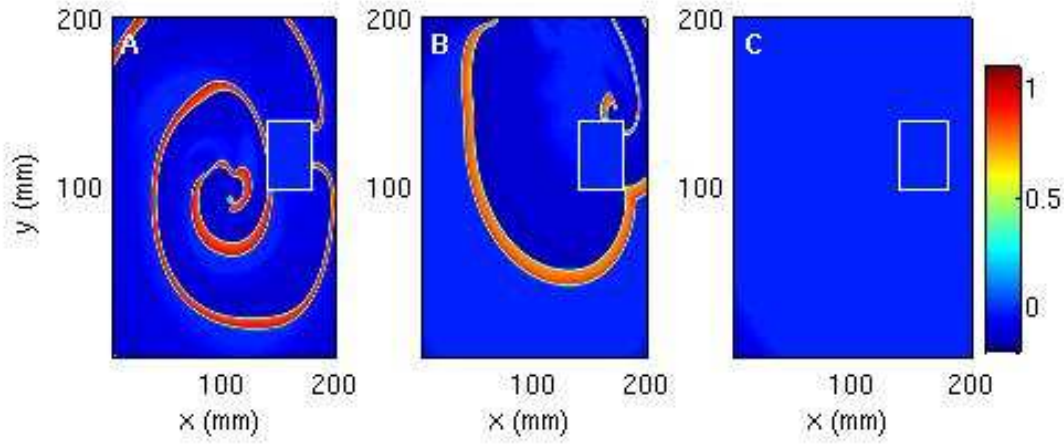

Spiral wave moves away from the medium in presence of the obstacle. When a square obstacle of side 40 mm is placed in the medium such that its lower-left corner is at (x =100 mm, y=140 mm) the the spiral moves away from the medium. A, B and C shows snapshots at time 1100 ms, 1650 ms and 2750 ms respectively.

Obstacle: Luo-Rudy Model, ST

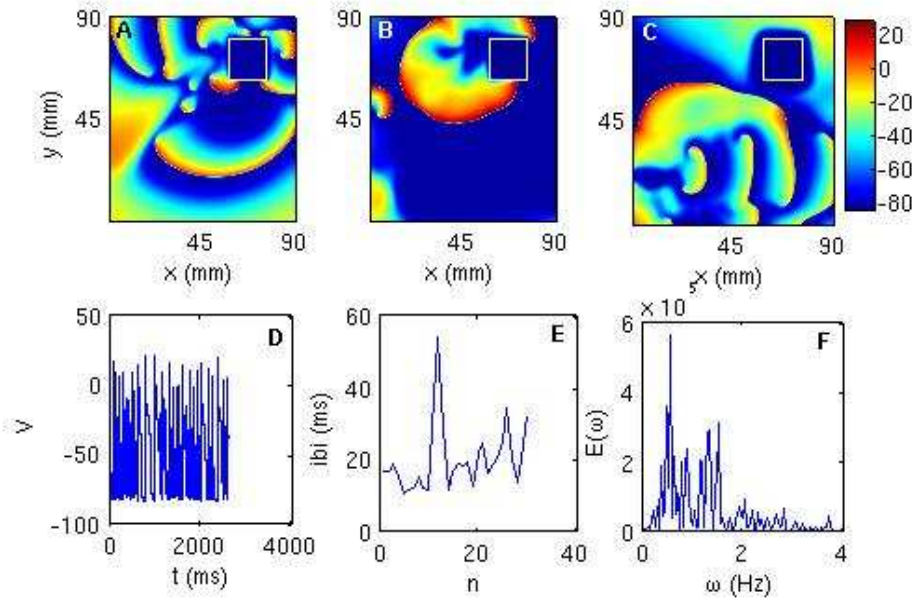

An obstacle of side l=18mm is placed at ($x = 58.5$ mm, $y = 63$ mm). The spiral turbulence persist in this case. A,B, and C shows snap shots taken at 200, 600, and 1000 ms respectively. D, E, and F show the local time series, interbeat interval, and powerspectrum calculated from a sample of 261 424 iterations.

Obstacle: Luo-Rudy Model, RS

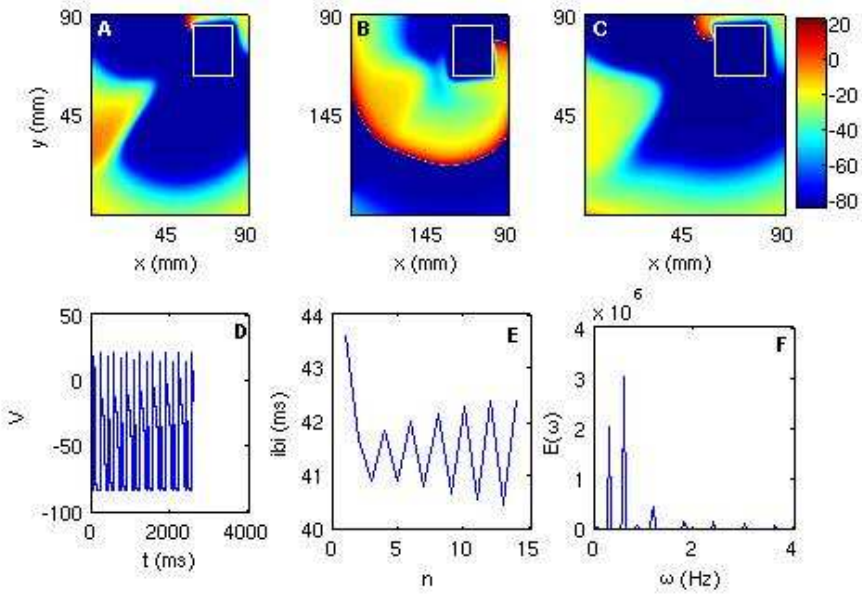

Obstacle of side l=18mm is placed at ($x = 58.5$ mm, $y = 63$ mm). The spiral anchores to the obstacle. A,B, and C shows snap shots taken at 200, 600, and 1000 ms respectively. D, E, and F show the local time series (taken from (x=45 mm, y=45 mm), interbeat interval, and powerspectrum calculated from a sample of 261 424 iterations.

Obstacle: Luo-Rudy Model, NS

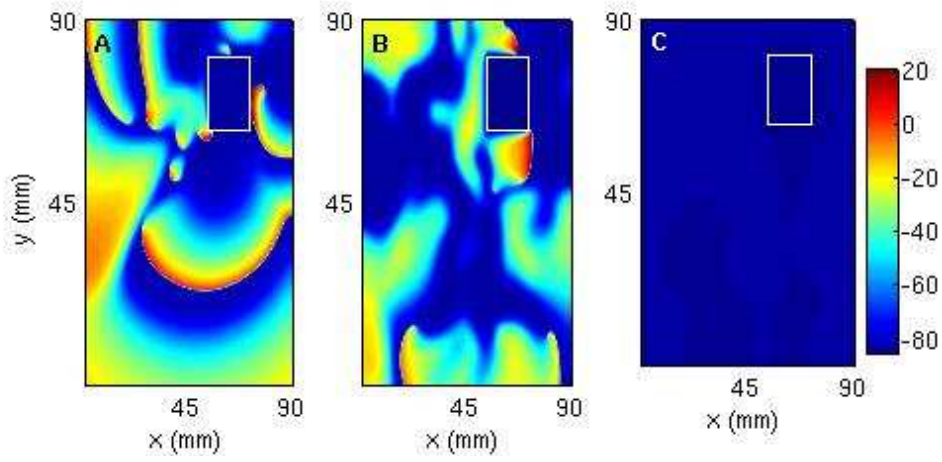

Spiral moving away from simulation domain because of the obstacle at ($x = 54$ mm,$y = 63$ mm). A,B, and C shows snap shots taken at 200, 600, and 1000 ms respectively.

Obstacle: redPB Model, RS

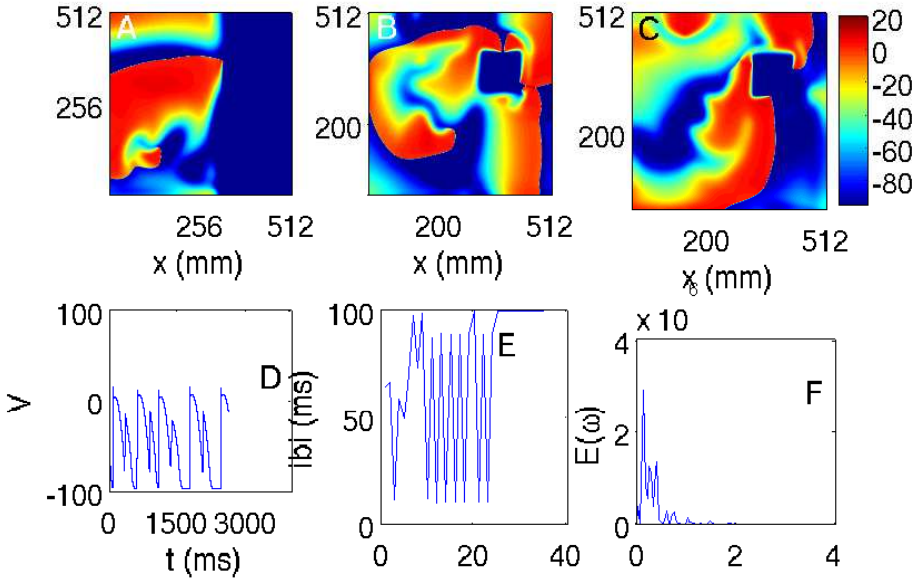

Obstacle of side l=18mm is placed at ($x = 67.5$ mm, $y = 72$ mm). The spiral anchors to the obstacle. A,B, and C shows snap shots taken at 200, 600, and 1000 ms respectively. D, E, and F show the local time series (taken from (x=45 mm, y=45 mm)), interbeat interval, and powerspectrum calculated from a sample of 261 424 iterations.

Animations

Square obstacle, VF
Square obstacle, VT
Square obstacle, NS
Two obstacles, VF
Two obstacles, VT
Two obstacles, NS
3D, ST
3D, RS
3D, NS

Stability Diagram

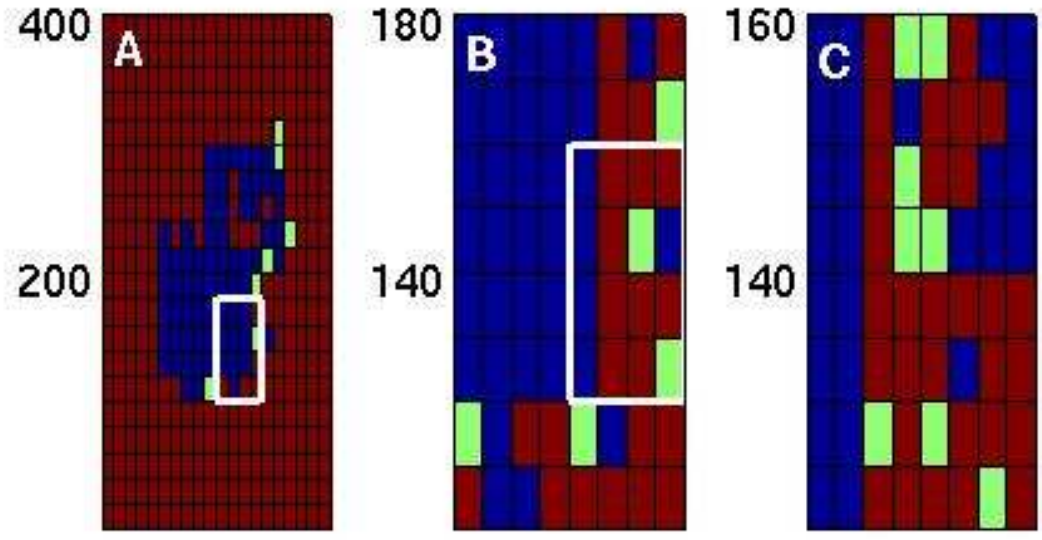

The colour of each small square indicates the final state of the system: red indicates spiral turbulence, blue a single anchored spiral, and green a quiescent state with no spirals, when the position of the lower-left hand corner of the obstacle coincides with that of the small square.

Ionic Inhomogeneities

- How do other kinds of heterogeneities in cardiac tissue affect spiral-wave dynamics ?
- The role of ionic heterogeneities in the system.
- Ionic heterogeneities can arise from ischemia, chronic heart failure or even from genetic disorders.
- They typically affect APD, and its timescales. They can also change the system from periodic to quasiperiodic and chaotic states.

Changing ϵ_1 in Panfilov Model

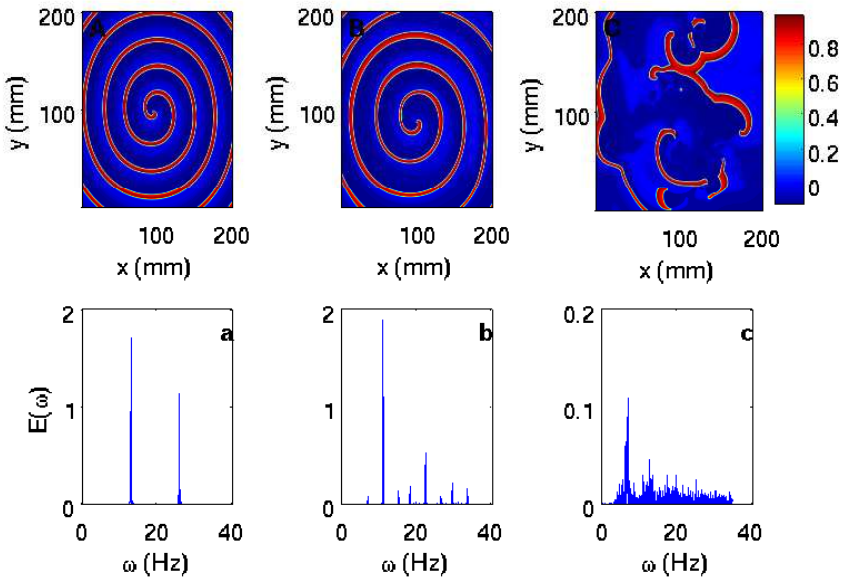

Figure shows the snap shots of V values after 3300 ms and associated powerspectra for different values of ϵ_1. (A) When ϵ_1=0.03; Note that there is only fundamental frequency in the powerspectrum corresponding to Hz indicating periodic spiral wave dynamics. (B) When ϵ_1=0.02, there are two independent fundamental frequencies indicating quasiperiodic nature of the spiral-wave dynamics. (C) When ϵ_1=0.01, the spiral waves break up and power spectrum is broad, indicating spatiotemporally chaotic dynamics.

Changing ϵ_1 in Panfilov Model

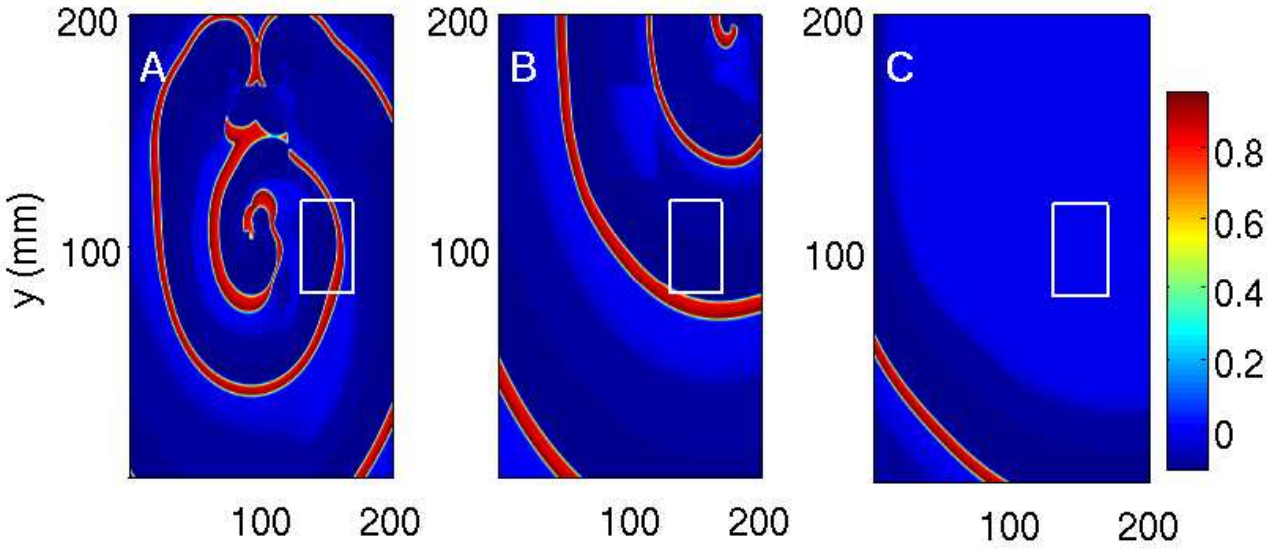

With ϵ_1^{out}=0.01 and ϵ_1^{in}=0.02, and ihomogeneity placed at (130 mm, 80 mm) spiral moves away from the medium. The above snap shots are taken at 1100 ms (A), 1650 ms (B) and 2200 ms (C).

Changing ϵ_1 in Panfilov Model

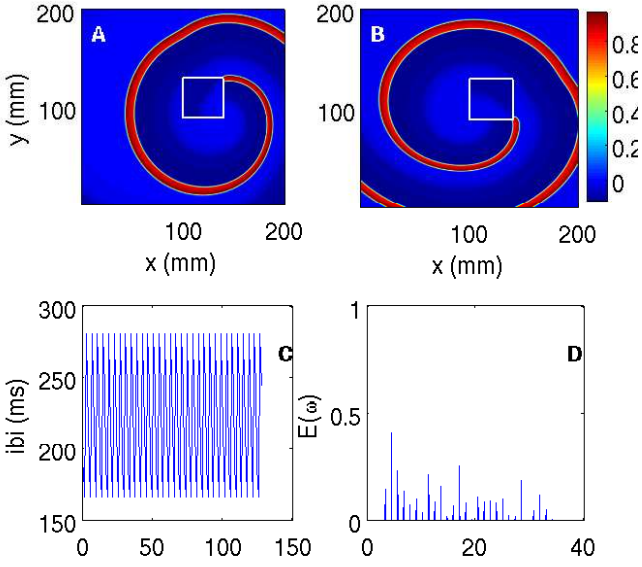

The Spiral wave gets anchored to the inhomogeneity. Here ϵ_1^{out}=0.01 and ϵ_1^{in} = 0.02. The inhomogeneity is placed at (100 mm, 90 mm). Though the spiral gets anchored note that the period of spiral wave is not constant, and exhibits quasiperiodic behaviour.

Conclusions

- VF: breakup of spiral/scroll waves induced by reentrant activity.
- Spiral turbulence is a spatiotemporally chaotic phenomenon in Panfilov, BR and LR models.
- The durations of chaotic transients depend on system size (small mammals are less likely to get heart attacks than large mammals).
- Spiral breakup in these models can be controlled by low-amplitude pulses.

Conclusions

- Our simulations show that cardiac arrhythmias depend sensitively on the shape, size, and positions of conduction inhomogeneities in ventricular tissue.
- This must arise because of a fractal basin that separates the domain of attraction of VF from those of VT and quiescent behaviour.
- Our work provides a natural explanation for the large variety of experimental results.

Conclusions

- Ionic and timescale heterogeneities also result in spiral suppression, anchoring, and complex spiral wave dynamics.
- Optimal anti-tachycardia pacing and defibrillation protocols might well have to be tailor made for different patients (as is done already to some extent).